Chemistry
A European
Journal

Chemistry Europe
European Chemical Societies Publishing

Accepted Article

Title: Kinetics and Mechanism of the Gold-Catalyzed Hydroamination of 1,1-Dimethylallene with N-Methylaniline

Authors: Ross Widenhoefer, Robert Harris, Kohki Nakafuku, Alethea Duncan, Robert Carden, and jacob timmerman

To be cited as: *Chem. Eur. J.* 10.1002/chem.202100741

Link to VoR: https://doi.org/10.1002/chem.202100741

WILEY-VCH

10.1002/chem.202100741

WILEY-VCH

FULL PAPER

Kinetics and Mechanism of the Gold-Catalyzed Hydroamination of 1,1-Dimethylallene with *N*-Methylaniline

Robert J. Harris, Kohki Nakafuku, Alethea N. Duncan, Robert G. Carden, Jacob C. Timmerman, and Ross A. Widenhoefer*

ABSTRACT. The mechanism of the intermolecular hydroamination of 3-methyl-1,2-butadiene (**1**) with *N*-methylaniline (**2**) catalyzed by (IPr)AuOTf has been studied employing a combination of kinetic analysis, deuterium labelling studies, and *in situ* spectral analysis of catalytically active mixtures. The results of these and additional experiments are consistent with a mechanism for hydroamination involving reversible, endergonic displacement of *N*-methylaniline from $[(IPr)Au(NHMePh)]^+$ (**4**) by allene to form the cationic gold π-*C1,C2*-allene complex $[(IPr)Au(\eta^2\text{-}H_2C{=}C{=}CMe_2)]^+$ (**I**) which is in rapid, endergonic equilibrium with the regioisomeric π-*C2,C3*-allene complex $[(IPr)Au(\eta^2\text{-}Me_2C{=}C{=}CH_2)]^+$ (**I'**). Rapid and reversible outer-sphere addition of **2** to the terminal allene carbon atom of **I'** to form gold vinyl complex $(IPr)Au[C(=CH_2)CMe_2NMePh]$ (**II**) is superimposed on slower addition of **2** to terminal allene carbon atom of **I** to form gold vinyl complex $(IPr)Au[C(=CMe_2)CH_2NMePh]$ (**III**). Selective protodeauration of **III** releases *N*-methyl-*N*-(3-methylbut-2-en-1-yl)aniline (**3a**) with regeneration of **4**. At high conversion, gold vinyl complex **II** is competitively trapped by an $(IPr)Au^+$ fragment to form the cationic bis(gold) vinyl complex $\{[(IPr)Au]_2[C(=CH_2)CMe_2NMePh]\}^+$ (**6**).

Introduction

Cationic gold(I) complexes have emerged over the past decade as highly active catalysts for the π-activation and subsequent functionalization of C–C multiple bonds,[1] notably for the cycloisomerization of 1,n-enynes[2] and the hydrofunctionalization of C–C multiple bonds.[3] The utility of cationic gold(I) complexes in these transformations can be traced to the high electrophilicity and low oxophilicity of the 12-electron $(L)Au^+$ fragment,[4] which leads to high reactivity coupled with good functional group compatibility.[1-3] Within this broad family of gold(I)-catalyzed π-activation processes, the gold(I)-catalyzed hydrofunctionalization of allenes has received particular attention owing to the diverse range of nucleophiles that participate in these transformations[5] and the potential for diastereo-[6] and enantioselective transformations.[7] Indeed, gold(I)-catalyzed allene hydrofunctionalization has been applied to good effect in a number of complex molecule syntheses.[8]

[a] Dr. R. J. Harris, Dr. J C. Timmerman, K. Nakafuku, S. Liu, R. G. Carden, Dr. A. N. Duncan, Prof. Dr. R. A. Widenhoefer
Department of Chemistry
Duke University
French Family Science Center, Durham, North Carolina, USA
E-mail: rwidenho@chem.duke.edu

Supporting information for this article is given via a link at the end of the document.

The proliferation of gold(I)-catalyzed allene hydrofunctionalization processes has likewise spurred interest in the mechanisms of these processes.[9] Along with insight gained from computational studies,[10,11] experimental studies have led to the synthesis of a number of potentially relevant intermediates including cationic gold π-allene complexes,[12,13] neutral mono(gold) vinyl complexes[14] and cationic bis(gold) vinyl complexes.[15,16] Similarly, stereochemical analyses of the gold(I)-catalyzed hydrofunctionalization of allenes with a diverse range of nucleophiles have consistently established the net *anti*-addition of the H–X bond of the nucleophile across the C=C bond of the allene, consistent with outer-sphere pathways for C–X bond formation.[17-21]

Despite the significant progress made in the synthesis and interrogation of potential intermediates in gold(I)-catalyzed allene hydrofunctionalization, there remains a dearth of information regarding the behavior of these potential intermediates under catalytic conditions, particularly in the context of intermolecular allene hydrofunctionalization. Mechanistic analysis of the gold(I)-catalyzed intramolecular hydroarylation[22] and hydroalkoxylation[23-25] of allenes and the related intramolecular hydroalkoxylation of alkynes[26,27] have established mechanisms involving turnover-limiting protodeauration with or without the involvement of off-cycle bis(gold) vinyl complexes. Toste and Goddard have likewise reported the mechanistic analysis of the gold(I)-catalyzed intermolecular hydroamination of 1,7-diphenylhepta-3,4-diene with methyl carbazate and proposed a mechanism involving turnover-limiting isomerization of a gold η^2-allene complex to a gold η^1-allylic cation transition state on the basis of computational and kinetic data.[28] However, as we have previously noted,[13,29] ambiguity regarding the nature of the catalyst resting state(s) in this system precludes the drawing of firm mechanistic conclusions from these kinetic data.

In response to limited experimental information regarding the mechanisms of gold(I)-catalyzed allene hydrofunctionalization, we have recently reported the kinetic and mechanistic analysis of the gold(I)-catalyzed intermolecular hydroalkoxylation of 3-methyl-1,2-butadiene (**1**) with 1-phenylpropanol catalyzed by (IPr)AuOTf.[29] These experiments supported a mechanism involving endergonic displacement of triflate from (IPr)AuOTf with **1** followed by irreversible, outer-sphere addition of alcohol to the resulting gold π-*C1,C2*-allene complex $[(IPr)Au(\eta^2\text{-}H_2C{=}C{=}CMe_2)]^+$ (**I**) (Scheme 1, eq 1). The microscopic rate constants controlling the formation and consumption of **I** were of similar magnitude, such that the reaction order varied depending on the absolute and relative concentrations of **1** and alcohol (eq 1). Under conditions of excess allene **1**, the reaction rate displayed first-order rate dependence on [ROH] and between zero- and first-order rate dependence on [**1**], while under conditions of excess alcohol, the reaction rate displayed first-

10.1002/chem.202100741

order rate dependence on [**1**] and zero-order rate dependence on [ROH].

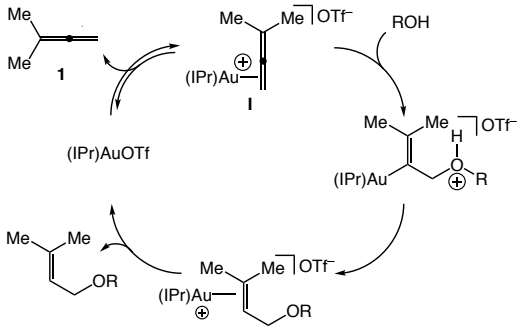

Scheme 1. Mechanism of gold(I)-catalyzed hydroalkoxylation of allene **1**.

$$rate = \frac{k_1 k_2[\mathbf{1}][\mathrm{ROH}][Au]_{tot}}{k_{-1} + k_1[\mathbf{1}] + k_2[\mathrm{ROH}]} \quad \text{Eq. (1)}$$

We targeted gold(I)-catalyzed allene hydroalkoxylation for initial kinetic investigation believing this transformation to be representative of the gold(I)-catalyzed hydrofunctionalization of allenes with weakly-binding nucleophiles. We sought to gain a similar understanding of the mechanisms of the gold(I)-catalyzed intermolecular hydrofunctionalization of allenes with more basic and potentially strongly binding nucleophiles. To this end, we have investigated the kinetics and mechanism of the gold(I)-catalyzed hydroamination of 3-methyl-1,2-butadiene (**1**) with *N*-methylaniline (**2**; Scheme 2) and herein we provide a full account of these investigations.

Results and Discussion

Kinetics of the Hydroamination of 1 with 2. Toward the elucidation of the mechanism of the gold(I)-catalyzed hydroamination of allenes with aryl amines, we focused our efforts on the hydroamination of 3-methyl-1,2-butadiene (**1**) with *N*-methylaniline (**2**) catalyzed by (IPr)AuOTf, which displays both high efficiency and high regioselectivity for the formation of the terminally-disubstituted allylic amine **3a** (**3a**:**3b** ≥97:3; Scheme 2).[30] Similarly, the single component catalyst (IPr)AuOTf was employed to avoid any potential complications associated with the presence of silver salts.[31] In an initial experiment, a solution of **1** (1.7 M), **2** (0.17 M), anthracene (70 mM; internal standard), and a catalytic amount of (IPr)AuOTf (8.35 mM; 5 mol %) in dioxane at 40 °C was analyzed periodically by HPLC. A plot of [**2**] versus time was linear to >3 half-lives with a pseudo-zero-order rate constant of 1.47 ± 0.05 × 10^{-5} M s^{-1} (Figure 1, Table 1, entry 1), which established zero-order dependence of the rate on *N*-methylaniline concentration; a plot of [**3a**] versus time was likewise linear with a pseudo-zero-order rate constant indistinguishable from that determined from a plot of [**2**] versus time.[32]

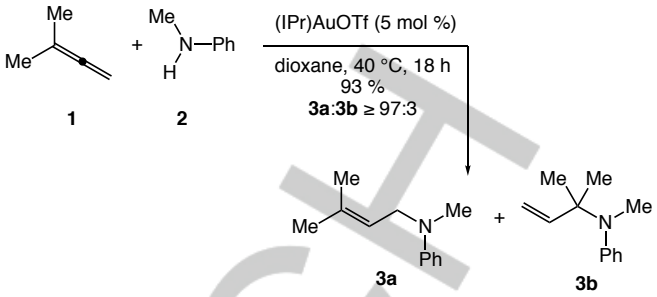

Scheme 2. Gold-catalyzed hydroamination of **1** with N-methylaniline.

Table 1. Pseudo-zero-order rate constants for the hydroamination of **1** with **2** (0.17 M) catalyzed by (IPr)AuOTf in dioxane at 40 °C.

Entry	[**1**] (M)	[(IPr)AuOTf] (mM)	(10^5)k_{obs} (s^{-1})
1	1.7	8.35	1.47 ± 0.05
2	1.7	4.34	0.71 ± 0.02
3	1.7	16.0	3.2 ± 0.1
4	0.83	8.13	0.87 ± 0.04
5	3.8	8.13	3.15 ± 0.09
6	4.5	8.13	3.9 ± 0.1
7[a]	1.7	8.24	1.20 ± 0.07

[a] *N*-methylaniline-*N*-*d* (**2**-*N*-*d*, 92% *d*) was used in this reaction.

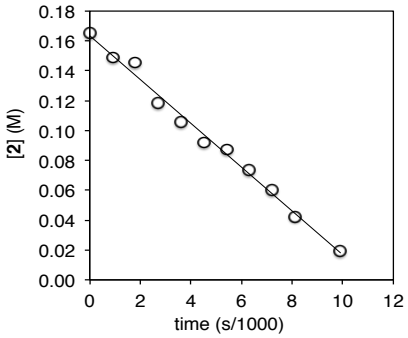

Figure 1. Plot of [**2**] versus time for the hydroamination of **1** (1.7 M) with **2** (0.17 M) catalyzed by (IPr)AuOTf (8.35 mM) in dioxane at 40 °C.

To determine the dependence of the rate of hydroamination on catalyst concentration, pseudo-zero-order rate constants were determined for the gold-catalyzed reaction of **2** (0.17 M) with **1** (1.7 M) as a function of [(IPr)AuOTf] from 0 to 16 mM (Table 1, entries 1-3). A plot of k_{obs} versus catalyst concentration was linear (Figure 2), which established the first-order dependence of the rate on catalyst concentration. To determine the dependence of the rate of hydroamination on allene concentration, pseudo-zero-order rate constants were determined for the reaction of **2** (0.17 M) with **1** catalyzed by [(IPr)AuOTf] (~8 mM) as a function of

10.1002/chem.202100741

allene concentration from 0.83 to 4.5 M (Table 1, entries 1, 4-6). A plot of the corresponding pseudo-first-order rate constants k ($k = k_{obs}$/[cat]) versus [**1**] was linear (Figure 3), which established the first-order dependence of the rate on allene concentration and overall the second-order rate law rate = k'[**1**][(IPr)AuOTf] where k' = 1.08 ± 0.05 × 10^{-3} M^{-1} s^{-1} ($\Delta G^{\ddagger}_{313K}$ = 22.6 kcal mol^{-1}).

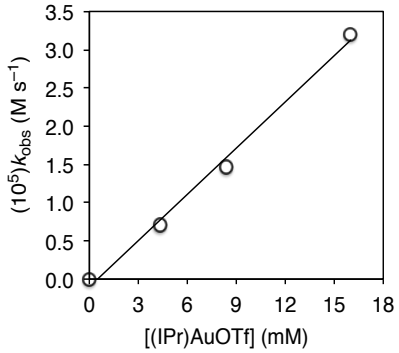

Figure 2. Plot of pseudo-zero-order rate constants versus catalyst concentration for the hydroamination of **1** (1.7 M) with **2** (0.17 M) catalyzed by (IPr)AuOTf (0-16 mM) in dioxane at 40 °C.

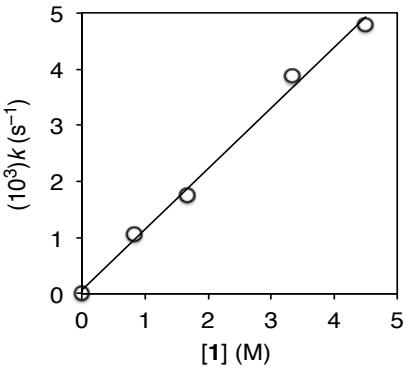

Figure 3. Plot of pseudo-first-order rate constants ($k = k_{obs}$/[cat]) versus allene concentration for the hydroamination of **1** (0-5 M) with **2** (0.17 M) catalyzed by (IPr)AuOTf (8.2 mM) in dioxane at 40 °C.

To gain insight into the potential involvement of a proton transfer process in a kinetically relevant step in the gold-catalyzed hydroamination of **1** with **2**, we evaluated the kinetic isotope effect (KIE) resulting from deuterioamination of **1** with *N*-deuterio-*N*-methylaniline (**2**-*N*-*d*). To this end, reaction of **1** (1.7 M) with **2**-*N*-*d* (0.17 M, 92% *d*) catalyzed by (IPr)AuOTf (8.13 mM) in dioxane at 40 °C formed **3a**-d_1 with 68% deuterium incorporation exclusively at the vinylic position (Scheme 3). The corresponding plot of [**2**] versus time was linear with a pseudo-zero-order rate constant of 1.20 ± 0.07 × 10^{-5} s^{-1} (Table 1, entry 7). Comparison of the corresponding pseudo-first-order rate constant with that determined for the hydroamination of **1** with **2** provides a deuterium KIE of k_H/k_D = 1.22 ± 0.08.

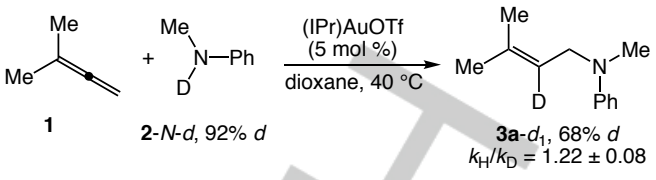

Scheme 3. Gold-catalyzed deuterioamination of **1** with N-methylaniline-d_1.

Reversibility of Hydroamination. The selective formation of the terminally disubstituted allylic amine **3a** in preference to the less-stable terminally unsubstituted allylic amine **3b** raises the possibility that **3a** is formed under catalytic conditions via the secondary isomerization of **3b**. Indeed, gold(I) complexes are known to catalyze the 1,3-transposition of allylic ethers in the presence of alcohols.[33] However, periodic ^{1}H NMR analysis of a solution of **2** (0.15 M), **1** (1.0 M) and (IPr*)AuOTf (IPr* = IPr-1-$^{13}C_1$; 7.5 mM) in dioxane-d_8 at 60 °C revealed the slow, steady accumulation of trace amounts of **3b** (~3% of the reaction mixture at 95% conversion), which is not consistent with **3b** as an intermediate in the formation of **3a**. Indeed, when a 1:1 mixture of **3b** and **2** and a catalytic amount of (IPr)AuOTf was heated at 40 °C in dioxane, no detectable consumption of **3b** or formation of **3a** was observed after 12 h by GC analysis (Scheme 4). Taken together, these experiments rule out **3b** as an intermediate in the gold(I)-catalyzed hydroamination of **1** with **2** to form of **3a**.

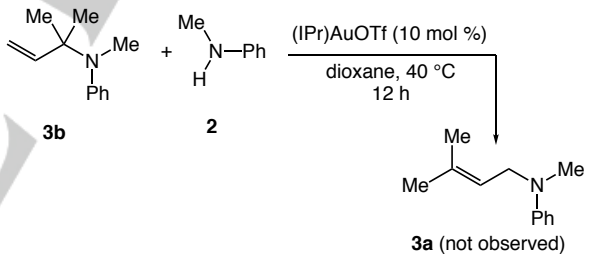

Scheme 4. Gold-catalyzed reaction of **3b** with *N*-methylaniline rules out **3b** as an intermediate in the formation of **3a**.

In situ Spectroscopic Analysis of Hydroamination. A series of experiments were performed to gain insight into the resting state(s) and relevant equilibria in the gold-catalyzed hydroamination of **1** with **2**. In one experiment, a solution of **1** (1.2 M), **2** (0.17 M), and the ^{13}C-labelled gold complex (IPr*)AuOTf (IPr* = IPr-1-$^{13}C_1$; 18 mM) in dioxane-d_8 was monitored periodically by ^{13}C NMR spectroscopy at 25 °C. The resonance at δ 168.9 corresponding to the carbene carbon atom of *N*-methylaniline complex [(IPr*)Au(NHMePh)]$^+$ (**4**-$^{13}C_1$) was observed within the first ~5% conversion and was the exclusive carbene-containing species observed through ~80% conversion (Figure 4).[34] At higher (~90%) conversion, a new resonance at δ 187.8 appeared and accounted for ~20% of the carbene-containing species. This resonance did not correspond to the gold triflate complex (IPr)AuOTf (δ 162.8), the gold π-*C1,C2*-allene complex **I** (δ 184.2),[12,34] or the gold-product complex [(IPr)Au(η^1-NMePhCH$_2$C=CMe$_2$)]$^+$ (**5**; δ 166.4).[34] Rather, the

10.1002/chem.202100741

spectroscopy and behaviour of this complex was most consistent with the terminally-unsubstituted bis(gold) vinyl complex {[(IPr*)Au]$_2$[C(=CH$_2$)CMe$_2$NMePh]}$^+$ (**6**-$^{13}C_2$) (see below).

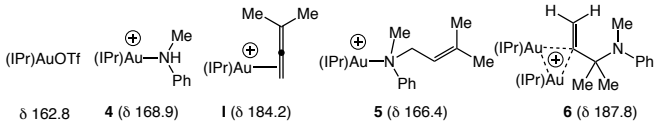

Figure 4. Potential intermediates in the gold-catalyzed hydroamination of **1** with **2** along with the diagnostic ^{13}C NMR chemical shifts of the C1-carbene carbon atom in dioxane-d_8 at 25 °C.[34]

A number of additional experiments were conducted to further clarify the relative binding affinities of **1**, **2**, and **3a** to the twelve-electron gold fragment (IPr)Au$^+$ and to provide insight into the structure and reactivity of **6**. In one experiment, a large excess of **1** (1.1 M) was added to a solution of (IPr*)AuOTf (33 mM) in dioxane-d_8 (Scheme 5). ^{13}C NMR analysis at 25 °C revealed quantitative conversion to the gold π-allene complex **I**-^{13}C (δ 184.2).[35] Addition of **2** (1.0 equiv) to this solution led to immediate (~2 min) and quantitative conversion of **I**-^{13}C to **4**-1-$^{13}C_1$, while ^1H NMR analysis revealed no detectable concentrations of free **2** and a small amount of **3a**, presumably due to employment of a slight excess of **2**.[36-38] From these observations and assuming that 10% of both **I**-^{13}C and **2** would have been detected in the ^{13}C and ^1H NMR spectra, respectively, we can assign a lower limit to the equilibrium constant for the conversion of **I** and **2** to **4** and **1** of K_{eq} = [**4**][**1**]/[**I**][**2**] ≥ 3 × 10^5. Furthermore, the rapid and quantitative formation of **4** from the reaction of **I** with **2** establishes the reversible formation of **I** from **4** under catalytic conditions.

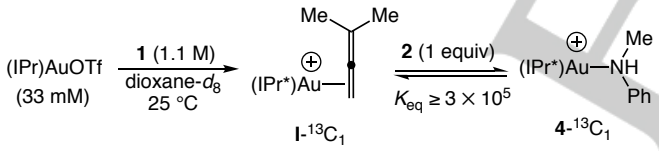

Scheme 5. Stoichiometric reaction of **I**-^{13}C ([Au] = 33 mM) with **2** in dioxane-d_8 at 25 °C (IPr* = IPr-1-^{13}C).

In a second experiment, **2** (1 equiv) was added to a solution of (IPr*)AuOTf (34 mM) in dioxane-d_8 at 25 °C. ^{13}C NMR analysis revealed the immediate and quantitative formation of **4**-$^{13}C_1$ (Scheme 6). The resulting solution was treated with excess **1** (0.50 M) and analysed by ^{13}C NMR spectroscopy at 25 °C, which revealed no detectable formation of **I**-$^{13}C_1$, consistent with the much higher binding affinity of **2** to gold relative to **1**. However, periodic ^{13}C NMR analysis of the solution revealed the quantitative conversion of **4**-$^{13}C_1$ to **6**-$^{13}C_2$ over the course of 110 min ($t_{1/2}$ = ~15 min). Periodic ^1H NMR analysis of the solution over this same time period revealed the appearance of resonances corresponding to protonated product **3a**•H$^+$ [δ 5.20 (br t, J = 7.0 Hz, 1 H), 4.04 (br d, J = 7.2 Hz, 2 H), 3.06 (br s, 3 H)],[39] which accounted for ~50% of the reaction mixture after 110 min. Periodic ^1H NMR analysis also revealed the appearance of a 1:1 ratio of resonances at δ 5.07 (br d, J = 4.4 Hz) and 4.32 (br d, J = 4.5 Hz), assigned to the terminal vinyl protons of **6**-$^{13}C_2$, which grew in concomitantly with the δ 187.8 resonance of **6**-$^{13}C_2$ in the ^{13}C NMR spectrum, ultimately accounting for ~25% of the reaction mixture. Upon complete consumption of **4**-$^{13}C_1$ (110 min), ^1H NMR analysis revealed the significant broadening of the resonances corresponding to **3a**•H$^+$ and the appearance of resonances corresponding to allylic amine **3b** [δ 5.93 (dd, J = 10.4, 17.2 Hz), 5.12 (dd, J = 17.2, 1.6 Hz), 4.87 (dd, J = 10.4, 1.6 Hz)], which accounted for ~25% of the reaction mixture (Scheme 6).

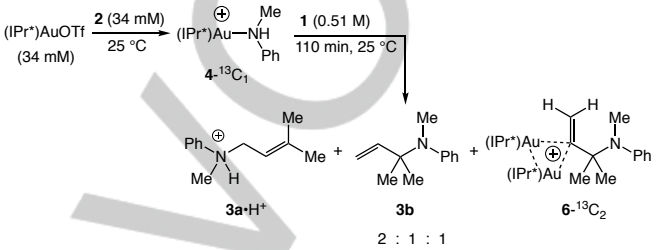

Scheme 6. Stoichiometric reaction of **4**-$^{13}C_1$ with **1**.

In a third experiment, a solution of **6**-$^{13}C_2$ in dioxane-d_8 was generated in a manner similar to that described in the preceding paragraph and the solution was evaporated to dryness, redissolved in dioxane-d_8, and analysed by NMR spectroscopy. ^{13}C NMR analysis revealed a 1.8:1 ratio of C1-carbene resonances at δ 187.8 corresponding to **6**-$^{13}C_2$ and δ 166.4 corresponding to the gold-**3a** adduct **5**-$^{13}C_1$, while ^1H NMR analysis revealed a ~2:1:1 mixture of **3a**•H$^+$, **5**-$^{13}C_1$, and **6**-$^{13}C_2$ (Scheme 7). Addition of **2** (~1 equiv) to this solution led to immediate disappearance of **6**-$^{13}C_2$ and **5**-$^{13}C_1$ to form **4**-$^{13}C_1$ as the exclusive carbene containing species as determined by ^{13}C NMR analysis and the formation of a 2.8:1.0:2.4 mixture of **3a**, **2**, and **4**-$^{13}C_1$ and traces of **3b** as determined by ^1H NMR analysis (Scheme 7). ^1H and ^{13}C NMR analysis of the reaction mixture also provided a lower limit for the equilibrium constant for the conversion of **5** and **2** to **4** and **3a** (i.e. the relative binding affinity of **2** relative to **3a**) of K_{eq} = [**4**][**3a**]/[**5**][**2**] ≥ 80, assuming that >5% of **5** would have been detected in the ^{13}C NMR spectrum. The failure of the reaction of **6**-$^{13}C_2$ with **2** to form significant quantities of **3b** established that **6**-$^{13}C_2$ is not predisposed to the formation of **3b**.

10.1002/chem.202100741

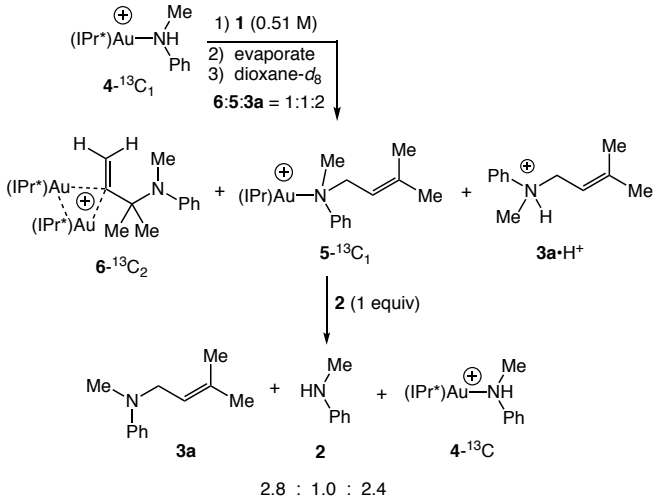

Scheme 7. Reaction of **4**-$^{13}C_1$ with excess **1** followed by evaporation and dissolution in dioxane-d_8 to form a mixture of **6**-$^{13}C_2$, **5**-$^{13}C_1$, and **3a**•H^+ and subsequent reaction with **2**.

Assignment of 6 as a bis(gold) vinyl complex. All of our experimental observations are consistent with the assignment of complex **6** as the terminally unsubstituted bis(gold) vinyl complex $\{[(IPr)Au]_2[C(=CH_2)CMe_2NMePh]\}^+$. First, both the chemical shift and peak separation of the ^{1}H NMR resonances at δ 5.07 (br d, J = 4.4 Hz) and δ 4.32 (br d, J = 4.5 Hz) assigned to the vinylic resonances of **6** and the chemical shift of the ^{13}C carbene resonance of **6** (δ 187.8) are consistent with known bis(gold) vinyl complexes generated via gold-mediated allene hydrofunctionalization.[15,22,25,40] Second, the terminally unsubstituted allylic amine **3b**, formed from the reaction of **4** with **1** in the absence of **2** (Scheme 6) is the anticipated product generated via protodeauration of **6** or, more likely, protodeauration of the corresponding mono(gold) vinyl complex **II** (Scheme 8). Third, although neither the spectroscopy of **6** nor its conversion to **3b** distinguish between a terminally unsubstituted bis(gold)- or mono(gold) vinyl complex, bis(gold) vinyl complexes are known to be highly resistant toward protodeauration, in sharp contrast to the facile protodeauration of mono(gold) vinyl complexes.[15,22,25,40] Therefore, the observed stability of **6** in the presence of the anilinium salt **3a**•H^+ (~35 mM) argues strongly against **6** as a mono(gold) vinyl complex but is fully consistent with a bis(gold) vinyl complex. Fourth, although (mono)gold vinyl complexes are known to bind strongly to the twelve-electron $(L)Au^+$ fragment, under catalytic conditions the mono(gold) vinyl complex **II** would complete with the strong binding ligand **2** for available $(IPr)Au^+$. Therefore, the observed formation of **6** only under conditions of low [**2**] under both catalytic and stoichiometric conditions and the rapid decomposition of mixtures of **6** and **3a**•H^+ (~35 mM) upon addition of **2** are fully consistent with the formulation of **6** as a bis(gold) vinyl complex. In addition, the formation of **3a**•H^+ concurrently with **6** under stoichiometric conditions strongly suggests that **6** exists largely in the non-protonated form, consistent with the diminished basicity of the nitrogen atom of **6** relative to **3a** owing to the proximal positive charge present on the bis(gold) fragment of **6**.

Proposed Mechanism of Hydroamination. The mechanism for the hydroamination of **1** with **2** catalyzed by (IPr)AuOTf depicted in Scheme 8 is consistent with all our experimental observations. Associative, endergonic displacement of **2** from gold *N*-methylaniline complex **4** with allene **1** would form the gold π-*C1,C2*-allene complex **I**, which is in rapid, endergonic equilibrium ($\Delta G^{\ddagger} \approx 10$ kcal/mol; $\Delta G \geq 2$ kcal/mol) with the regioisomeric gold π-*C2,C3*-allene complex $[(IPr)Au(\eta^2\text{-}Me_2C{=}C{=}CH_2)]^+$ (**I'**).[12] Rapid and reversible outer-sphere[17-22] addition of **2** to the terminal allene carbon atom of **I'** would form the gold vinyl complex **II**, whereas slower addition of **2** to the terminal allene carbon atom of **I** would form the gold vinyl complex **III**. Irreversible protodeauration of **II** would release allylic amine **3b** in the minor reaction pathway while more facile irreversible protodeauration of **III** would form **3a** via gold π-alkene complex **IV**[41] in the major pathway, in both cases with regeneration of **4**. At high conversion where the concentration of **2** is low, gold vinyl complex **II** is competitively trapped by a $(IPr)Au^+$ fragment to form the bis(gold) vinyl complex **6**, which accumulates under reaction conditions and presumably functions as an off-cycle catalyst reservoir.[24]

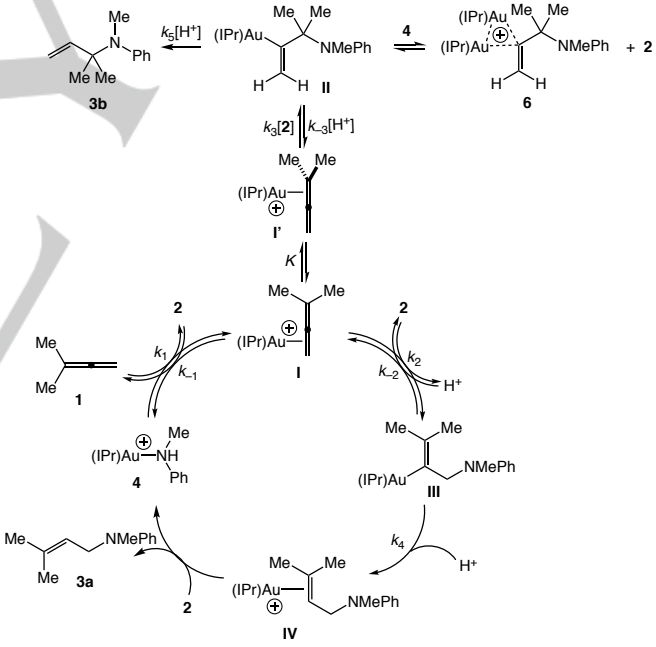

Scheme 8. Proposed mechanism for the gold(I)-catalyzed hydroamination of **1** with **2** catalyzed by (IPr)AuOTf.

The rapid formation of gold *N*-methyl aniline complex **4** upon treatment of **I** with **2** under stoichiometric conditions (Scheme 5) and the much higher binding affinity of **2** for the $(IPr)Au^+$ fragment relative to **1** ($K_{eq} \geq 3 \times 10^5$) establishes the reversible, endergonic ($\Delta G_{298K} \geq 7.5$ kcal/mol) formation of **I** from **4** under catalytic conditions (Scheme 8). Note also that although the mechanism depicted in Scheme 8 invokes intermolecular protodeauration, we

have no evidence that would distinguish between inter- and intramolecular pathways for protodeauration.[42-45]

The accumulation of **6** under catalytic conditions at high conversion coupled with the formation of **3b** in only trace amounts (≤3%) under catalytic conditions points to the rapid and reversible formation of gold vinyl complex **II** under catalytic conditions. However, the absence of a large deuterium KIE for the deuterioamination of **1** with **2**-*N*-*d* (k_H/k_D = 1.22 ± 0.08) coupled with the reversible formation of **I** from **4** argues against a scenario involving rapid and reversible formation of both **II** and **III** followed by turnover-limiting protodeauration of **III** under Curtin-Hammett conditions, which would be expected to display a large primary KIE. Rather, these observations are more consistent with a scenario involving rapid and reversible formation of **II** superimposed on much slower formation of **III**. The small but significant deuterium KIE points to a kinetically relevant protodeauration step, suggesting that the energy barrier for the protodeauration of **III** is not significantly higher than is the energy barrier for formation of **III** from **I** and **2** (see below). The failure to form significant amounts of **3b** under catalytic conditions can therefore be attributed to the less favorable protodeuaration of **II** relative to **III** and not to the preferential attack of aniline on the terminal allene carbon atom of gold π-*C1,C2*-allene complex **I** relative to attack of aniline on the terminal allene carbon atom of gold π-*C2,C3*-allene complex **I'**.

Both the kinetically preferred addition of **2** to the more substituted allene terminus of **I'** relative to the addition of **2** to the less substituted allene terminus of **I** and the more facile protodeauration of **III** relative to **II** are consistent with the general reactivity trends displayed by gold(I) σ- and π-complexes. For example, the kinetically preferred addition of **2** to the more substituted allene terminus of **I'** is in accord with the established polarization of π-bonds upon coordination to (L)Au$^+$[16] and also with the high Markovnikov selectivity displayed by the gold(I)-catalyzed hydroamination of alkenes and alkynes.[3] Likewise, the more facile protodeauration of the terminally disubstituted vinyl complex **III** relative to the terminally unsubstituted vinyl complex **II** is fully consistent with both experimental and computational analyses of protodeauration, which have established the increasing rate of protodeauration with the increasing electron density of the σ-bound ligand.[41,46,47] For example, we have previously shown that treatment of the terminally unsubstituted δ-allenyl alcohol **7a** with a stoichiometric mixture of (**P1**)AuOTf [**P1** = P(*t*-Bu)$_2$*o*-biphenyl] and Et_3N led to isolation of the corresponding terminally unsubstituted gold vinyl complex **8a** (Scheme 9).[48] In contrast, the analogous reaction of the terminally disubstituted allenyl alcohol **7b** with (**P1**)AuOTf and Et_3N formed none of the anticipated vinyl gold complex but instead led to exclusive formation of the vinyl ether **8b**, pointing to the highly facile protodeauration in these latter case (Scheme 9).[48]

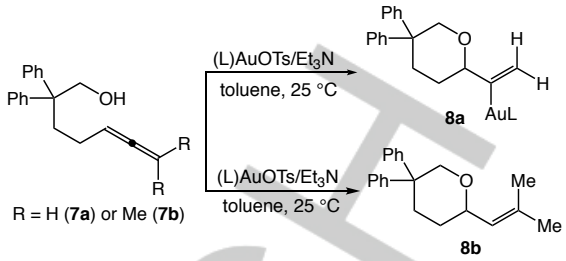

Scheme 9. Disparate reactivity of terminally substituted and terminally disubstituted δ-allenyl alcohols toward protodeauration.

Kinetic Model for Hydroamination. We sought to derive differential rate equations for the mechanism depicted in Scheme 8 that would describe the kinetic behaviour of catalytic hydroamination under conditions where aggregation of intermediate **II** to form **6** was negligible (0 - ~90% convn), which constitutes the concentration regime where the bulk of our kinetic data was determined. Under these conditions, (1) gold–*N*-methylaniline complex **4** is the only gold-containing species that accumulates under catalytic conditions ([Au]$_{tot}$ = [**4**]), (2) formation of allylic amine **3b** is negligible ($k_5 \approx 0$), as is aggregation of **II**, and (3) protodeauration (**III** → **IV**), and hence hydroamination, is irreversible.[42-45] Under these restrictions, application of the Bodenstein (steady-state) approximation to intermediates **I**, **II**, and **III** generates the rate expression depicted in eq 2. This rate equation predicts first-order rate dependence on [catalyst] and [**1**], zero-order rate dependence on [**2**], and the potential for a deuterium KIE for the deuterioamination of **1**, depending on the magnitude of the microscopic rate constant k_4 relative to k_{-2}. For example, under conditions of turnover-limiting protodeauration (i.e. $k_4 << k_{-2}$), rate equation 2 simplifies to that depicted in eq 3, which predicts that the primary deuterium KIE will reach its maximum. Conversely, under conditions of turnover-limiting C–N bond formation (i.e. $k_{-2} = 0$) rate equation 2 simplifies to rate equation 4, which predicts that the primary deuterium KIE will fall to zero.

$$rate = \frac{k_1 k_2 k_4 [\mathbf{1}][Au]_{tot}}{k_{-1}k_{-2} + k_{-1}k_4 + k_2 k_4} \qquad \text{Eq. (2)}$$

$$rate = K_1 K_2 k_4 [\mathbf{1}][Au]_{tot} \;\; when \;\; k_4 << k_{-2} \;\; \text{Eq. (3)}$$

$$rate = \frac{k_1 k_2 [\mathbf{1}][Au]_{tot}}{k_{-1} + k_2} \;\; when \;\; k_{-2} = 0 \quad \text{Eq. (4)}$$

The experimental rate law determined for the gold(I)-catalyzed hydroamination of **1** with **2** (rate = k[**1**][Au]$_{tot}$) and the small but significant deuterium KIE observed for deuterioamination of **1** with **2**-*N*-*d* (k_H/k_D = 1.22 ± 0.08) is consistent with the kinetic scenario described by rate equation 2 and approaches the limiting scenario described by rate equation 4 involving turnover-limiting C–N bond formation. However, the small primary KIE observed for deuterioamination indicates that

the limiting condition $k_4 << k_{-2}$ associated with rate expression 7 is not fully met, suggesting that the transition state energy for protodeauration is not significantly lower than is that for C–N bond formation.

The kinetics of the gold-catalyzed hydroamination of **1** with **2** at high conversion (≥90%) become largely intractable owing to (1) the aggregation of two reactive intermediates (**II** and **4**), (2) the accumulation of two different catalytic species (**4** and **6**) under reaction conditions, and (3) the conversion-dependent change in catalyst composition. However, consideration of the equilibria involved in the formation of **6** from **4** suggests that at high conversion the reaction rate should approach first-order dependence on [**2**] and half-order dependence on [cat] while maintaining first-order dependence on [**1**]. It is therefore not surprising that we observed no such deviations from the rate law: rate = k[**1**][Au]$_{tot}$ in our kinetic analyses seeing that the onset of catalyst aggregation to form **6** (>80% convn) was very near the end range at which kinetic data was collected and because **6** accounted for only ~20% of the catalyst composition at 90% conversion.

Relationship to Other Gold(I)-Catalyzed Hydrofunctionalization Processes. As noted in the Introduction, we have recently reported the kinetic/mechanistic analysis of the hydroalkoxylation of **1** with 1-phenylpropanol catalyzed by (IPr)AuOTf in toluene.[29] Worth noting are two of the key differences in the catalytic/kinetic behavior of hydroamination of allene **1** with **2** relative to the hydroalkoxylation of allenes with aliphatic alcohols that can be traced directly to the greater binding affinity and basicity of **2** relative to 1-phenylpropanol. Firstly, in the case of catalytic hydroalkoxylation, complexation of alcohol to gold was insignificant and the gold triflate complex (IPr)AuOTf and the gold π-allene complex **I** both accumulated under reaction conditions, leading to rate dependence on both [allene] and [alcohol] that varied between zero- and first-order depending on reaction conditions. Conversely, in the case of hydroamination, the binding affinity of **2** so exceeds that of both OTf^- and **1** that the gold aniline complex **4** represented to sole catalyst resting state prior to the onset of catalyst aggregation, leading to zero-order rate dependence on [**2**] and first-order rate dependence on [allene]. Secondly, in the case of hydroalkoxylation, protodeauration was fast under all conditions, whereas, protodeauration was kinetically relevant in the case of the hydroamination of **1** with **2** (although not rate-limiting), presumably due to the greater basicity of the aryl amines relative to alcohols and ethers. In the case of hydroalkoxylation of **1** with 1-phenylpropanol, the significantly more facile protodeauration relative to C–O bond formation precluded the accumulation of bis(gold) vinyl complexes.

As was likewise noted in the Introduction, Toste and Goddard have reported a combined experimental/computational analysis of the intermolecular hydroamination of 1,7-diphenyl-3,4-heptadiene with methyl carbazate to form *N*-allylic carbazate **9** catalyzed by $(Ph_3P)AuNTf_2$ in nitromethane at 45 °C (Scheme 10).[28] Some additional comments regarding this mechanism are warranted in lieu of the results disclosed in this work. The authors invoked a "two-step, no intermediate" mechanism involving turnover-limiting isomerization of a gold η^2-allene complex to a gold η^1-allylic cation transition state that is trapped by methyl carbazate either prior to or after progression to the achiral η^1-allylic cation. Experimentally, this mechanism was supported by (1) the rate law: rate = k[allene][Au]$_{tot}$ with ~zero-order rate dependence on methyl carbazate concentration and (2) assignment of the gold π-allene complex $[(Ph_3P)Au(\eta^2\text{-}PhCH_2CH_2C{=}C{=}CCH_2CH_2Ph)]^+$ (**10**) as the catalyst resting state as determined by *in situ* ^{31}P NMR analysis and independent syntheses.

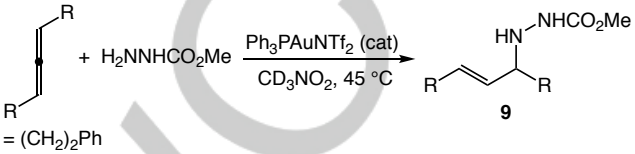

Scheme 10. Gold-catalyzed hydroamination of 1,7-diphenyl-3,4-heptadiene with methyl carbazate. [28]

Widenhoefer and Brooner subsequently demonstrated that the species assigned by Toste and Goddard as π-allene complex **10** is rather the catalyst decomposition product $[(PPh_3)_2Au]^+$,[13] and without clear identification of the catalyst resting state(s) in the gold-catalyzed hydroamination of 1,7-diphenyl-3,4-heptadiene with methyl carbazate, the zero-order rate dependence on methyl carbazate concentration need not be attributed to turnover-limiting allene activation. For example, if the known gold methyl carbazate complex $[(PPh_3)Au(H_2NNHCO_2Me)]^+$ NTf_2^- (**11**)[28] were the predominant species that accumulated under catalytic conditions, the experimentally determined rate law (rate = k[allene][Au]$_{tot}$) would be inconsistent with the proposed mechanism involving turnover-limiting allene activation, but would be consistent with a mechanism involving reversible formation of **10** followed by either irreversible, turnover-limiting outer-sphere attack of methyl carbazate or reversible addition of carbazate to **10** followed by turnover-limiting intramolecular protodeauration, analogous to the mechanisms proposed for the gold-catalyzed hydroamination of **1** with **2** depicted in Scheme 8.

We sought to gain additional information regarding the distribution of gold-containing species present under reaction conditions for the gold-catalyzed hydroamination of 1,7-diphenyl-3,4-heptadiene with methyl carbazate. Unfortunately, as was reported by Toste and Goddard,[28] ^{31}P NMR analysis of catalytic mixtures of 1,7-diphenyl-3,4-heptadiene, methyl carbazate, and $Ph_3PAuNTf_2$ at 45 °C showed no discernible peaks in the spectral range δ 25 - 40 that would reveal the accumulation of **10** (δ 36)[13] and/or **11** (δ 28),[28] presumably due to rapid intermolecular ligand exchange, nor would ^{31}P NMR analysis likely distinguish between methyl carbazate complex **11** and the gold allylic carbazate complex **12** (δ 28) owing to the nominal dispersion of the ^{31}P NMR resonances of these complexes (Figure 5).[49] However, in the slow exchange regime (–25 °C) in CD_3NO_2, the binding affinity of methyl carbazate exceeds that of 1,7-diphenyl-3,4-heptadienene by a factor of 70 and of **9** by a factor of 20 (Scheme 11). Because we do not know the temperature dependence of these equilibria, no definitive conclusions can be drawn regarding the distribution

of catalytic species under reaction conditions (CD_3NO_2, 45 °C). Nevertheless, these observations do support a scenario involving gold methyl carbazate complex **11** as the predominant species present under catalytic conditions, particularly given the conditions of excess methyl carbazate employed in the kinetic analyses,[28] and therefore, support a mechanism analogous to that depicted in Scheme 8 in favor of the "two-step, no intermediate" mechanism initially proposed for this transformation.

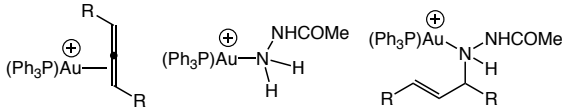

10 [R = $(CH_2)_2Ph$] **11** **12** [R = $(CH_2)_2Ph$]

Figure 5. Potential intermediates in the gold-catalyzed hydroamination of 1,7-diphenyl-3,4-heptadiene with methyl carbazate.

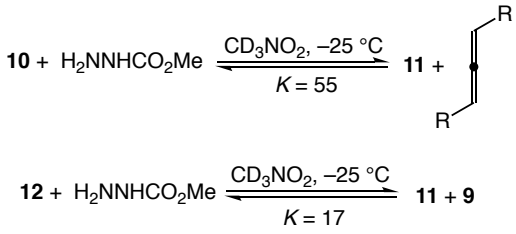

Scheme 11. Key equilibria in the gold-catalyzed hydroamination of 1,7-diphenyl-3,4-heptadiene with methyl carbazate.

Conclusions

In summary, we have investigated the kinetics and mechanism of the hydroamination of 3-methyl-1,2-butadiene (**1**) with *N*-methylaniline (**2**) in dioxane. All of our data are consistent with the mechanism depicted in Scheme 8 involving endergonic displacement of **2** from the gold *N*-methyl aniline complex $[(IPr)Au(NHMePh)]^+$ (**4**) with **1** to form the cationic gold π-allene complex **I**. Rapid and reversible outer-sphere addition of **2** to the terminal allene carbon atom of **I'** forms gold vinyl complex **II** whereas slower addition of **2** to the terminal carbon atom of **I** forms gold vinyl complex **III**. Selective protodeauration of **III** releases the allylic amine product **3a** and regenerates **4**. The small but significant deuterium KIE observed for deuterioamination of **1** with **2**-*N*-*d* points to a kinetic scenario that approaches turnover-limiting formation of **III** with a small but significant kinetic contribution of protodeauration. Under conditions where the concentration of **2** is low, such as at high conversion, gold vinyl complex **II** is competitively trapped by $(IPr)Au^+$ to form the bis(gold) vinyl complex **6**, which accumulates under reaction conditions and accounts for ~20% of the available catalyst at 90% conversion.

The gold-catalyzed hydrofunctionalization of differentially substituted allenes has been shown to lead selectively to either the linear or branched allylic product resulting from addition of the nucleophile to the less substituted or more substituted allene terminus, respectively.[3] However, the origins of the nucleophile, solvent, and ligand-dependent regioselectivity of the gold(I)-catalyzed hydrofunctionalization of differentially substituted allenes remain obscure and there has been no unifying mechanism that might both account for the disparate regioselectivity of these transformations and be in accord with the established reactivity patterns of gold σ- and π-complexes. Although gold-catalyzed allylic transposition has been invoked to account for selective formation of the linear hydrofunctionalization product,[11] our results both herein and in the context of hydroalkoxylation rule out this possibility.[29] Rather, the mechanism for regiocontrol proposed herein involving rapid and reversible attack of nucleophile at the more substituted allene terminus superimposed on slower addition to the less substituted allene terminus coupled with more facile protodeauration of the terminally disubstituted gold vinyl complex might better account all the observations made in the context of gold-catalyzed allene hydrofunctionalization. According to such a mechanism, subtle changes in the relative rates of formation, consumption, and protodeauration of the gold vinyl intermediates could lead to complete inversion in regiochemistry of otherwise similar systems.

Experimental Section

Experimental details including synthetic preparations, compound characterization data, kinetic procedures, and kinetic plots can be found in the Supporting Information.

Acknowledgements

We acknowledge the NSF (CHE-1465209) for support of this research. RGC was supported through a GAANN fellowship (P200A150114).

Conflict of interest

The authors declare no conflict of interest.

Keywords: hydroamination • mechanism • kinetics • gold • allene

[1] a) Y. Li, W. Li, J. Zhang, *Chem. Eur. J.* **2017**, *23*, 467 – 512; b) A. Quintavalla, M. Bandini, *ChemCatChem* **2016**, *8*, 1437-1453; c) J. Miróand, C. del Pozo, *Chem. Rev*. **2016**, *116*, 11924−11966; d) M. N. Hopkinson, A. Tlahuext-Aca, F. Glorius, *Acc. Chem. Res*. **2016**, *49*, 2261−2272; e) P. H. S. Paioti, A. Aponick, *Top. Curr. Chem*. **2015**, *357*, 63–94; f) A. M. Asiri, A. S. K. Hashmi, *Chem. Soc. Rev*. **2016**, *45*, 4471-4503; g) L. Liu, J. Zhang, *Chem. Soc. Rev*. **2016**, *45*, 506-516; h) S. Shin, *Top. Curr. Chem*. **2015**, *357*, 25–62; i) V. Michelet, *Top. Curr. Chem*. **2015**, *357*, 95–132.

[2] a) R. Dorel, A. M. Echavarren, *Chem. Rev*. **2015**, *115*, 9028−9072; b) Y. C. Lee, K. Kumar, *Isr. J. Chem.* **2018**, *58*, 531-556; c) E. Jiménez-Núnêz, A. M. Echavarren, *Chem. Rev*. **2008**, *108*, 3326–3350; d) A. S.

K. Hashmi, T. M. Frost, J. W. Bats, Highly Selective Gold-Catalyzed Arene Synthesis. *J. Am. Chem. Soc*. **2000**, *122*, 11553-11554.

[3] a) R. Blieck, M. Taillefer, F. Monnier, *Chem. Rev*. **2020**, *120*, 13545−13598; b) C. Praveen, *Coord. Chem. Rev*. **2019**, *392*, 1–34; c) A. Quintavalla, M. Bandini. *ChemCatChem* **2016**, *8*, 1437-1453; d) A. Arcadi, in *Topics in Heterocyclic Chemistry*, Bandini, M. Ed. Springer, 2016, pp 53-85; e) J. L. Mascareñas, F. López, in *Topics in Heterocyclic Chemistry*, M. Bandini, Ed. Springer, 2016, pp 1-52; f) N. Huguet, A. M. Echavarren, *Top. Organomet. Chem*. **2013**, *43*, 291-324; g) C. Winter, N. Krause, in *Modern Gold Catalyzed Synthesis*; A. S.K. Hashmi, F. D. Toste, Eds.; Wiley-VCH, 2012, pp 363-389; h) A. Corma, A. Leyva-Pérez, M. J. Sabater, *Chem. Rev*. **2011**, *111*, 1657–1712; i) H. C. Shen, *Tetrahedron* **2008**, *64*, 3885-3903; j) X. Han, R. A. Widenhoefer, *Eur. J. Org. Chem*. **2006**, 4555-4563.

[4] a) T. J. Brown, M. G. Dickens, R. A. Widenhoefer, *J. Am. Chem. Soc*. **2009**, *131*, 6350-6351; b) T. J. Brown, M. G. Dickens, R. A. Widenhoefer, *Chem. Commun*. **2009**, 6451–6453.

[5] a) N. Krause, C. Winter, *Chem. Rev*. **2011**, *111*, 1994-2009; b) N. Nishina, Y. Yamamoto, *Tetrahedron* **2009**, *65*, 1799–1808.

[6] a) N. T. Patil, *Chem. Asian J*. **2012**, *7*, 2186 – 2194; b) D. Campolo, S. Gastaldi, C. Roussel, M. P. Bertrand, M. Nechab, *Chem. Soc. Rev*. **2013**, *42*, 8434—8466.

[7] a) W. Zi, F. D. Toste, *Chem. Soc. Rev*. **2016**, *45*, 4567-4589; b) A. Pradal, P. Y. Toullec, V. Michelet, *Synthesis* **2011**, 1501-1514; c) S. Sengupta, X. Shi, *ChemCatChem* **2010**, *2*, 609-619; d) R. A. Widenhoefer, *Chem. Eur. J*. **2008**, *14,* 5382-5391.

[8] a) M. Rudolph, A. S. K. Hashmi, *Chem. Soc. Rev*. **2012**, *41*, 2448–2462; b) D. Pflästerer, A. S. K. Hashmi, *Chem. Soc. Rev*. **2016**, *45*, 1331-1367; c) Z. Liu, A. S. Wasmuth, S. G. Nelson, *J. Am. Chem. Soc*. **2006**, *128*, 10352-10353; d) R. M. Zeldin, F. D. Toste, *Chem. Sci*. **2011**, *2*, 1706-1709; e) R. W. Bates, M. R. Dewey, *Org. Lett*. **2009**, *11*, 3706-3708; f) Y. Sawama, Y. Sawama, N. Krause, *Org. Biomol. Chem*. **2008**, *6*, 3573-3579; g) V. M. Schmiedel, S. Stefani, H.-U. Reissig, *Beilstein J. Org. Chem*. **2013**, *9*, 2564-2569; h) O. F. Jeker, E. M. Carreira, *Angew. Chem., Int. Ed*. **2012**, *51*, 3474-3477; *Angew. Chem*. **2012**, *124*, 3531–3534. i) T.Okada, K. Sakaguchi, T. Shinada, Y. Ohfune, *Tetrahedron Lett*. **2011**, *52*, 5744-5746.

[9] a) W. Yang, A. S. K. Hashmi, *Chem. Soc. Rev*. **2014**, *43*, 2941-2955; b) A. S. K. Hashmi, L. Schwarz, J.-H. Choi, T. M. Frost, *Angew. Chem. Int. Ed. Engl*. **2000**, *39*, 2285-2288; *Angew. Chem*. **2000**, *112*, 2382– 2385.

[10] a) O. N. Faza, C. S. López, *Top. Curr. Chem*. **2015**, 357, 213-283; b) E. Soriano, I. Fernández, *Chem. Soc. Rev*. **2014**, *43*, 3041-3105; c) M.; Malacria, L. Fensterbank, V. Gandon, *Top. Curr. Chem.* **2011**, *302*, 157-182; d) B. Alcaide, P. Almendros, T. M. Campo, E. Soriano, J. Marco-Contelles, *Top. Curr. Chem*. **2011** *302*, 183-224; e) S. Montserrat, G. Ujaque, F. López, J. L. Mascarenãs, A. Lledós, *Top. Curr. Chem*. **2011**, *302*, 225-248; f) V. Gandon, G. Lemiére, A. Hours, L. Fensterbank, M. Malacria, *Angew. Chem. Int. Ed*. **2008**, *47*, 7534-7538; *Angew. Chem*. **2008**, *120*, 7644 –7648; g) S. Montserrat, H. Faustino, A. Lledós, J. L. Mascareñas, F. López, G. Ujaque, *Chem. Eur. J*. **2013**, *19*, 15248-15260; h) D. Benitez, E. Tkatchouk, A. Z. Gonzalez, W. A. Goddard, F. D. Toste, *Org. Lett*. **2009**, *11*, 4798-4801; i) R.-X. Zhu, D.-J. Zhang, J.-X. Guo, J.-L. Mu, C.-G. Duan, C.-B. Liu, *J. Phys. Chem. A* **2010**, *114*, 4689–4696.

[11] a) R. S. Paton, F. Maseras, *Org. Lett*. **2009**, *11*, 2237-2240; b) S. Muñoz-López, A. Couce-Rios, G. Sciortino, A. Lledós, G. Ujaque, *Organometallics* **2018**, *37*, 3543−3551.

[12] a) T. J. Brown, A. Sugie, M. G. Dickens, R. A. Widenhoefer, *Chem. Eur. J*. **2012**, *18*, 6959-6971; b) T. J. Brown, A. Sugie, M. G. Dickens, R. A. Widenhoefer, *Organometallics* **2010**, *29*, 4207-4209.

[13] R. E. M. Brooner, T. J. Brown, R. A. Widenhoefer, *Chem. Eur. J*. **2013**, *19*, 8276-8284.

[14] a) L.-P. Liu, B. Xu, M. S. Mashuta, G. B. Hammond, *J. Am. Chem. Soc*. **2008**, *130*, 17642-17643; b) L.-P. Liu, G. B. Hammond, *Chem.–Asian J*. **2009**, *4*, 1230-1236; c) Y. Shi, K. E. Roth, S. D. Ramgren, S. A. Blum, *J. Am. Chem. Soc*. **2009**, *131*, 18022-18023; d) L. N. dos Santos Comprido, J. E. M. N. Klein, G. Knizia, J. Kästner, A. S. K. Hashmi, *Chem. Eur. J*. **2017**, *23*, 10901 – 10905, and references therein.

[15] a) D. Weber, M. R. Gagne, *Top. Curr. Chem*. **2015**, *357*, 167-211; (b) A. Gómez-Suárez, S. P. Nolan, *Angew. Chem. Int., Ed*. **2012**, *51*, 8156-8159; *Angew. Chem*. **2012**, *124*, 8278– 8281.

[16] For additional reviews on intermediates generated in gold(I) catalysis with relevance to allene hydrofunctionalization see: a) L.-P. Liu, G. B. Hammond, *Chem. Soc. Rev*. **2012**, *41*, 3129-3139; b) C. Obradors, A. M. Echavarren, *Chem. Commun*. **2014**, *50*, 16-28; c) T. Lauterbach, A. M. Asiri, A. S. K. Hashmi, *Adv. Organomet. Chem*. **2014**, *62*, 261-297; d) B. Ranieri, I. Escofeta, A. M. Echavarren, *Org. Biomol. Chem*. **2015**, *13*, 7103-7118; e) A. C. Jones, *Top. Curr. Chem*. **2015**, *357*, 133-165; f) R. E. M. Brooner, R. A. Widenhoefer, *Angew. Chem. Int. Ed*. **2013**, *52*, 11714-11724; *Angew. Chem*. **2013**, *125*, 11930-11941; g) H. Schmidbaur, A. Schier, *Organometallics* **2010**, *29*, 2-23; h) M. A. Cinellu, in Modern Gold Catalyzed Synthesis, ed. A. S. K. Hashmi, D. F. Toste, Wiley-VCH, 2012, p. 153.

[17] a) Z. Zhang, R. A. Widenhoefer, *Org. Lett*. **2008**, *10*, 2079-2081; b) Z. Zhang, C. Liu, R. E. Kinder, X. Han, H. Qian, R. A. Widenhoefer, *J. Am. Chem. Soc*. **2006**, *128*, 9066-9073; c) B. Gockel, N. Krause, *Org. Lett*. **2006**, *8*, 4485-4488; d) Z. Zhang, R. A. Widenhoefer, *Angew. Chem., Int. Ed*. **2007**, *46*, 283-285; *Angew. Chem*. **2007**, *119*, 287-289; e) C. Winter, N. Krause, *Angew. Chem., Int. Ed*. **2009**, 48, 6339-6342; *Angew. Chem*. **2009**, *121*, 6457–6460; f) N. Morita, N. Krause, *Angew. Chem., Int. Ed*. **2006**, 45, 1897-1899; *Angew. Chem*. **2006**, *118*, 1930–1933; g) Z. Zhang, C. F. Bender, R. A. Widenhoefer, *J. Am. Chem. Soc*. **2007**, *129*, 14148-14149.

[18] Yamamoto established the net *anti*-addition of the N–H bond of aniline across the C=C bond of an allene under gold(III) catalysis, but nevertheless invoked an inner-sphere mechanism for this transformation, which necessitated the inclusion of the unprecedented E to Z isomerization of gold vinyl intermediate to account for preferential formation of the E allylic amine: N. Nishina, Y. Yamamoto, *Angew. Chem. Int. Ed*. **2006**, *45*, 3314 - 3317; *Angew. Chem*. **2006**, *118*, 3392–3395.

[19] Although Stradiotto initially proposed an inner-sphere mechanism to account for the net *syn*-addition in the the gold(I)-catalyzed hydroamination of alkynes with alkyl amines,[20] this proposal was subsequently repudiated by Zhdanko and Maier who demonstrated that the syn-addition product in the gold catalyzed hydroaminaton of alkyl amines with alkynes is generated via stereoisomerization of the gold iminium intermediate generated via net anti-addition of the N–H bond of the amine across the CC bond of the alkyne.[21]

[20] K. D. Hesp, M. Stradiotto, *J. Am. Chem. Soc*. **2010**, *132*, 18026 – 18029.

[21] A. Zhdanko, M. E. Maier, *Angew. Chem. Int. Ed*. **2014**, *53*, 7760–7764; *Angew. Chem*. **2014**, *126*, 7894– 7898.

[22] a) D. Weber, M. A. Tarselli, M. R. Gagné, *Angew. Chem., Int. Ed*. **2009**, *48*, 5733-5736; *Angew. Chem*. **2009**, *121*, 5843 –5846; b) D. Weber, M. R. Gagné, *Org. Lett*. **2009**, *11*, 4962-4965; c) D. Weber, M. R. Gagné, *Chem. Sci*. **2013**, *4*, 335-338.

[23] N. Cox, M. R. Uehling, K. T. Haelsig, G. Lalic, *Angew. Chem. Int. Ed*. **2013**, *52*, 4878-4882; *Angew. Chem*. **2013**, *125*, 4978-4982.

[24] T. J. Brown, D. Weber, M. R. Gagné, R. A. Widenhoefer, *J. Am. Chem. Soc*. **2012**, *134*, 9134-9137.

[25] T. J. Brown, R. E. M. Brooner, M. A. Chee, R. A. Widenhoefer, *Organometallics* **2016**, *35*, 2014−2021.

[26] a) A. Zhdanko, M. E. Maier, *Chem. Eur. J*. **2013**, *19*, 3932-3942; b) A. Zhdanko, M. E. Maier, *Organometallics* **2013**, *32*, 2000-2006; c) A. Zhdanko, M. E. Maier, *Chem. Eur. J*. **2014**, *20*, 1918-1930.

[27] See also: a) W. Wang, M. Kumar, G. B. Hammond, B. Xu, *Org. Lett.* **2014**, *16*, 636−639; b) W. Wang, G. B. Hammond, B. Xu, *J. Am. Chem. Soc.* **2012**, *134*, 5697−5705; c) L. Lempke, H. Sak, M. Kubicki, N. Krause, *Org. Chem. Front*. **2016**, *3*, 1514-1519.

[28] Z. J. Wang, D. Benitez, E. Tkatchouk, W. A. Goddard, F. D. Toste, *J. Am. Chem. Soc*. **2010**, *132*, 13064-13071.

[29] R. J. Harris, R. G. Carden, A. N. Duncan, R. A. Widenhoefer, *ASC Catal.* **2018**, *8*, 8941–8952.

[30] A. N. Duncan, R. A. Widenhoefer, *Synlett* **2010**, 419-422.

[31] a) A. Zhdanko, M. E. Maier, *ACS Catal.* **2015**, *5*, 5994−6004; b) D. Wang, R. Cai, S. Sharma, J. Jirak, S. K. Thummanapelli, N. G. Akhmedov, H. Zhang, X. Liu, J. L. Petersen, X. Shi, *J. Am. Chem. Soc*. **2012**, *134*, 9012−9019; c) A. Homs, I. Escofet, A. M. Echavarren, *Org. Lett.* **2013**, *15*, 5782−5785; d) M. Kumar, G. B. Hammond, B. Xu, *Org. Lett.* **2014**, *16*, 3452−3455; e) Y. Zhu, C. S. Day, L. Zhang, K. J. Hauser, A. C. Jones, *Chem. Eur. J*. **2013**, *19*, 12264 – 12271; f) L. Hu, M. C. Dietl, C. Han, M. Rudolph, F. Rominger, A. S. K. Hashmi, *Angew. Chem. Int. Ed*. **2021**, *60*, 10637 –10642; *Angew. Chem*. **2021**, *133*, 10731 –10737; g) Y. Yang, P. Antoni, M. Zimmer, K. Sekine, F. F. Mulks, L. Hu, L. Zhang, M. Rudolph, F. Rominger, A. S. K. Hashmi, *Angew. Chem. Int. Ed.* **2019**, *58*, 5129 –5133; *Angew. Chem*. **2019**, *131*, 5183 –5187.

[32] The regioisomeric allylic amines **3a** and **3b** were not distinguished by HPLC under these conditions.

[33] a) P. Mukherjee, R. A. Widenhoefer, *Chem. Eur. J*. **2013**, *19*, 3437–3444; b) A. Aponick, B. Biannic, *Synthesis* **2008**, 3356-3359; c) A. Aponick, C.-Y. Li, J. A. Palmes, *Org. Lett*. **2009**, *11*, 121-124; d) Aponick,; Li, C.-Y.; Biannic, B. *Org. Lett.* **2008**, *10*, 669-671; e) A. Aponick, B. Biannic, M. R. Jong, *Chem. Commun*. **2010**, *46*, 6849-6851; f) M.Bandini, M. Monari, A. Romaniello, M. Tragni, *Chem. Eur. J.* **2010**, *16*, 14272-14277; g) B. Biannic, A. Aponick, *Bielstein J. Org. Chem.* **2011**, *7*, 802-807; h) A. Aponick, B. Biannic, *Org. Lett*. **2011**, *13*, 1330-1333; i) T.Ghebreghiorgis, B. Biannic, B. H. Kirk, D. H. Ess, A. Aponick, *J. Am. Chem. Soc*. **2012**, *134*, 16307-16318; j) G. Barker, D. G. Johnson, P. C. Young, S. A. Macgregor, A.-L. Lee, *Chem. Eur. J*. **2015**, 21, 13748 – 13757; k) E. Coutant, P. C. Young, G. Barker, A.-L. Lee, *Beilstein J. Org. Chem*. **2013**, *9*, 1797–1806.

[34] Complex **I** has been previously synthesized.[12] Complexes **4** and **5** were synthesized independently and fully characterized (See Supporting Information).

[35] In non-polar solvents such as dioxane, the binding affinity of triflate to the fragment $(IPr)Au^+$ significantly exceeds that of **1**, which necessitates a large excess of **1** to quantitatively convert (IPr)AuOTf to **I**.[29]

[36] Isoprene was formed as a byproduct via gold-catalyzed isomerization of **1**,[37,38] but was not detected in the presence of **2**.

[37] T. J. Brown, B. D. Robertson, R. A. Widenhoefer, *J. Organomet. Chem*. **2014**, *758*, 25-28.

[38] a) X. Cheng, Z. Wang, C. D. Quintanilla, L. Zhang *J. Am. Chem. Soc*. **2019**, *141*, 3787−3791; b) X. Li, Z. Wang, X. Ma, P.-n. Liu, L. Zhang, *Org. Lett*. **2017**, *19*, 5744−5747; c) Z. Wang, Y. Wang, L. Zhang, *J. Am. Chem. Soc*. **2014**, *136*, 8887−8890.

[39] A. De Renti, B. Di Blasio, A. Panunzi, C. Pedone, A. Vitagliano *J. Chem. Soc., Dalton Trans*. **1978**, 1392-1397.

[40] T. J. Brown, D. Weber, M. R, Gagné, R. A. Widenhoefer, *J. Am. Chem. Soc.* **2012**, *134*, 9134–9137.

[41] L. N. dos Santos Comprido, J. E. M. N. Klein, G. Knizia, J. Kästner, A. S. K. Hashmi, *Chem. Eur. J*. **2017**, *23*, 10901 - 10905.

[42] Although H^+ is certainly present under catalytic conditions in the form of the ammonium salt **B**•H^+ [**B** = **2** or **3**], [**B**] is invariant throughout the course of the reaction prior to accumulation of **6** (i.e. $[\mathbf{B}]_t = [\mathbf{2}]_t + [\mathbf{3a}]_t = [\mathbf{2}]_0 = [\mathbf{3a}]_{inf}$) and the basicity of secondary and tertiary anilines varies by only a fraction of a pK_a unit.[43] For this reason, treating the source of proton as either H^+ or **B**•H^+ leads to indistinguishable rate equations. Furthermore, because H^+ (or **B**•H^+) is a co-reactant in both the forward and reverse reactions involving **III**, the reaction rate is invariant of [H^+] (or **B**•H^+). In a similar manner, a mechanism involving *N*-protonation of **III** followed by intramolecular protodeauration likewise produces an indistinguishable rate equation (See Supporting Information).

[43] The pK_a values for aniline, *N*-methylaniline, and *N,N*-dimethylaniline in water (DMSO) are 4.60 (3.72), 4.85 (2.76), and 5.16 (2.51), respectively.[44,45]

[44] N. F. Hall, M. R. Sprinkle, *J. Am. Chem. Soc*. **1932**, *54*, 3469.

[45] R. L. Benoit, M. J. Mackinnon, L. Bergeron, *Can. J. Chem*. **1981**, *59*, 1501.

[46] K. E. Roth, S. A. Blum, *Organometallics* **2010**, *29*, 1712–1716.

[47] a) R. BabaAhmadi, P. Ghanbari, N. A. Rajabi, A. S. K. Hashmi, B. F. Yates, A. Ariafard, *Organometallics* **2015**, *34*, 3186−3195; b) C. A. Gaggioli, G. Ciancaleoni, D. Zuccaccia, G. Bistoni, L. Belpassi, F. Tarantelli, P. Belanzoni, *Organometallics* **2016**, *35*, 2275−2285.

[48] T. J. Brown, R. E. M. Brooner, M. A. Chee, R. A. Widenhoefer, *Organometallics* **2016**, *35*, 2014−2021.

[49] See the Supporting Information for details.

10.1002/chem.202100741

WILEY-VCH

FULL PAPER

Entry for the Table of Contents

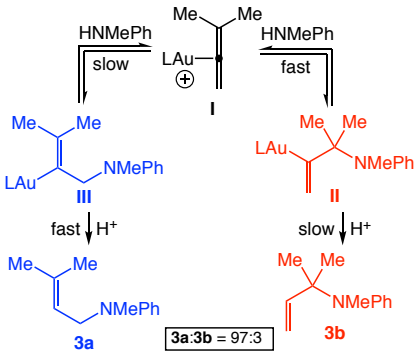

Kinetic and spectroscopic analysis of the gold-catalyzed hydroamination of 1,1-dimethylallene with *N*-methylaniline support a mechanism involving rapid and reversible addition of *N*-methylaniline to the more substituted terminus of gold π-allene complex **I** to form gold vinyl complex **II** superimposed on slower addition of *N*-methylaniline to the less substituted terminus of **I** to form gold vinyl complex **III**. Selective formation of the linear allylic amine **3a** is attributed to the more facile protodeauration of III relative to **II**.